

Title	Analysis of AlN/AlGaIn/GaN metal-insulator-semiconductor structure by using capacitance-frequency-temperature mapping
Author(s)	Shih, Hong-An; Kudo, Masahiro; Suzuki, Toshi-kazu
Citation	Applied Physics Letters, 101(4): 043501-1-043501-4
Issue Date	2012-07-24
Type	Journal Article
Text version	publisher
URL	http://hdl.handle.net/10119/12902
Rights	Copyright 2012 American Institute of Physics. This article may be downloaded for personal use only. Any other use requires prior permission of the author and the American Institute of Physics. The following article appeared in Hong-An Shih, Masahiro Kudo and Toshi-kazu Suzuki, Applied Physics Letters, 101(4), 043501 (2012) and may be found at http://dx.doi.org/10.1063/1.4737876
Description	

Analysis of AlN/AlGaIn/GaN metal-insulator-semiconductor structure by using capacitance-frequency-temperature mapping

Hong-An Shih, Masahiro Kudo, and Toshi-kazu Suzuki^{a)}

Center for Nano Materials and Technology, Japan Advanced Institute of Science and Technology (JAIST),
1-1 Asahidai, Nomi, Ishikawa 923-1292, Japan

(Received 7 June 2012; accepted 5 July 2012; published online 24 July 2012)

AlN/AlGaIn/GaN metal-insulator-semiconductor (MIS) structure is analyzed by using capacitance-frequency-temperature (C - f - T) mapping. Applying sputtering-deposited AlN, we attained AlN/AlGaIn/GaN MIS heterostructure field-effect transistors with much suppressed gate leakage currents, but exhibiting frequency dispersion in C - V characteristics owing to high-density AlN/AlGaIn interface states. In order to investigate the interface states deteriorating the device performance, we measured temperature-dependent frequency dispersion in the C - V characteristics. As a result, we obtained C - f - T mapping, whose analysis gives the activation energies of electron trapping, namely the interface state energy levels, for a wide range of the gate biases. This analysis method is auxiliary to the conventional conductance method, serving as a valuable tool for characterization of wide-bandgap devices with deep interface states. From the analysis, we can directly evaluate the gate-control efficiency of the devices. © 2012 American Institute of Physics.
[<http://dx.doi.org/10.1063/1.4737876>]

AlGaIn/GaN heterojunction field-effect transistors (HFETs)¹ have been extensively developed as promising devices for high-frequency and high-power applications. However, gate leakage current is a limiting factor for practical usage of these devices. In order to solve this problem, AlGaIn/GaN metal-insulator-semiconductor (MIS) HFETs, enabling effective reduction of the gate leakage currents, have been developed and studied. In particular, high-dielectric-constant (high- k) oxide materials, such as Al₂O₃ (Ref. 2) or HfO₂ (Refs. 3 and 4), have been investigated as a gate insulator of the MIS-HFETs. On the other hand, AlN is an important high- k non-oxide insulator possessing possible suitability for III-V device processing.^{5,6} In addition to AlN-passivated AlGaIn/GaN HFETs exhibiting good heat release properties^{7–12} due to the high thermal conductivity of AlN (~ 10 times higher than that of Al₂O₃),¹³ AlN/AlGaIn/GaN MIS-HFETs, where the AlN gate insulator was sputtering-deposited, have been investigated,^{7,14,15} owing to a possible high breakdown field $\gtrsim 10$ MV/cm (Refs. 16 and 17) and a high dielectric constant ~ 10 (Ref. 18) comparable to those of Al₂O₃. In particular, we showed significant suppression of gate leakage current, although frequency dispersion in the C - V characteristics for forward gate biases was observed.¹⁵ This dispersion is attributed to high-density AlN/AlGaIn interface mid-gap states leading to a gate-control impediment, which severely depresses the device performances. Such mid-gap states in GaN-based devices have been investigated by Terman method,^{19–21} conductance method,^{14,15,22–27} and deep level transient spectroscopy (DLTS).^{28–31} In the previous work, we employed the conductance method for analysis of capacitance-voltage-frequency (C - V - f) characteristics to investigate the AlN/AlGaIn interface state density and electron trapping time constant at room temperature.¹⁵ In this work, we propose an analysis

method using capacitance-frequency-temperature (C - f - T) mapping obtained from the temperature-dependent C - V - f characteristics. This method gives the activation energies of electron trapping, namely the interface state energy levels, for a much extended range of the gate biases, serving as an auxiliary tool to the conventional conductance method.

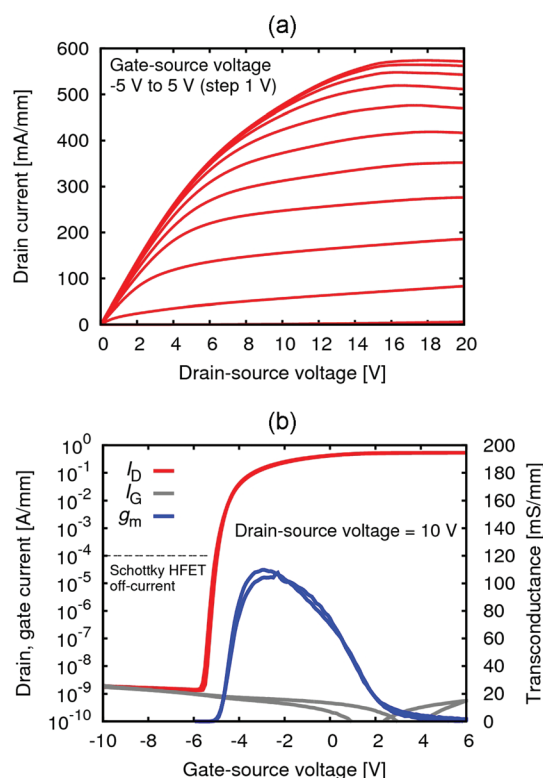


FIG. 1. Characteristics of the AlN/AlGaIn/GaN MIS-HFET. (a) Output characteristics. (b) Transfer characteristics, where drain current I_D , gate current I_G , and transconductance g_m were obtained under the gate voltage sweep of $-10 \text{ V} \rightarrow +6 \text{ V} \rightarrow -10 \text{ V}$.

^{a)} Author to whom correspondence should be addressed. Electronic mail: tosikazu@jaist.ac.jp.

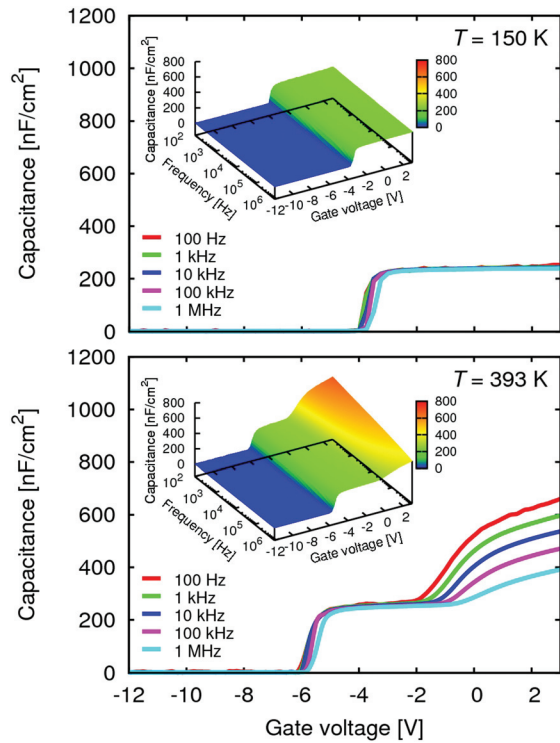


FIG. 2. C - V - f characteristics of the AlN/AlGaIn/GaN MIS structure at 150 K (above) and 393 K (below).

Moreover, from the interface state energy levels corresponding to a wide range of the gate biases, we can directly evaluate the gate-control efficiency of the devices.

We fabricated AlN/AlGaIn/GaN MIS-HFETs and MIS structures simultaneously using an $\text{Al}_{0.29}\text{Ga}_{0.71}\text{N}$ (25 nm)/GaIn (3000 nm) heterostructure obtained by metal-organic vapor phase epitaxy on sapphire(0001). Hall measurements of the heterostructure show an as-grown electron mobility of $1200 \text{ cm}^2/\text{V}\cdot\text{s}$ and a sheet electron concentration of $1.3 \times 10^{13} \text{ cm}^{-2}$. On the heterostructure, Ti/Al/Ti/Au Ohmic electrodes were formed and device isolation was achieved by B^+ implantation. On the AlGaIn surface cleaned by organic solvents, deionized water, and oxygen plasma ashing to remove surface organic contaminants, followed by oxide removal using Semicoclean (ammonium-based etchant), an AlN gate insulator of $\sim 19 \text{ nm}$ thickness was deposited by RF magnetron sputtering at room temperature with an AlN target in Ar-N_2 ambient. The formation of Ni/Au gate electrodes completed the device fabrication. The MIS-HFETs have the gate length of 250 nm, the source-gate spacing of 2 μm , the gate-drain spacing of 3 μm , and the gate width of 50 μm , while the MIS structures have the 100 $\mu\text{m} \times 100 \mu\text{m}$ gate electrode surrounded by the Ohmic electrode.

In Figs. 1(a) and 1(b), we show output and transfer characteristics of the fabricated MIS-HFET, respectively. Owing to good insulating properties of the AlN, gate leakage currents are significantly small, 10^{-9} A/mm range or less, for both reverse and forward gate biases. The small gate leakage currents lead to small drain off-currents shown in Fig. 1(b). However, we observe a rapid decrease in the transconductance towards forward gate biases, suggesting high-density AlN/AlGaIn interface states.

In order to investigate the AlN/AlGaIn interface states, we measured the C - V - f characteristics between the 100 $\mu\text{m} \times 100 \mu\text{m}$ gate electrode and the grounded Ohmic electrode surrounding the gate of the MIS structure at temperatures from 150 K to 393 K. Figure 2 shows the C - V - f characteristics at 150 K and 393 K. At 393 K, we observe a significant frequency dispersion for forward gate biases, which is attributed to electron trapping at interface states, while the frequency dispersion disappears at 150 K because of much longer electron trapping time constants. To characterize the interface states quantitatively, we carried out an analysis using the conductance method³² based on the equivalent circuit of the MIS structures depicted in the inset of Fig. 3 (top), with the insulator capacitance C_0 , the semiconductor capacitance C_s , the interface state capacitance C_i , and the interface state conductance G_i . Using the interface state density D_i and the electron trapping time constant τ , we obtain³³

$$C_i = \frac{q^2 D_i \arctan(\omega\tau)}{\omega\tau} \quad (1)$$

and

$$\frac{G_i}{\omega} = \frac{q^2 D_i \ln(1 + \omega^2\tau^2)}{2\omega\tau}, \quad (2)$$

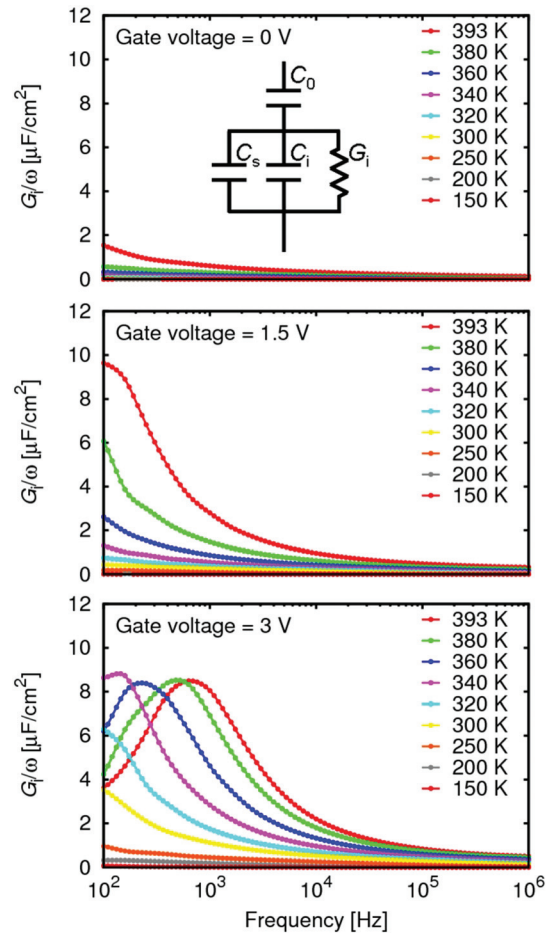


FIG. 3. Frequency dependence of G_i/ω for temperatures from 393 K to 150 K at gate voltages of 0 V (top), 1.5 V (middle), and 3 V (bottom). Top inset: the equivalent circuit of the MIS structures.

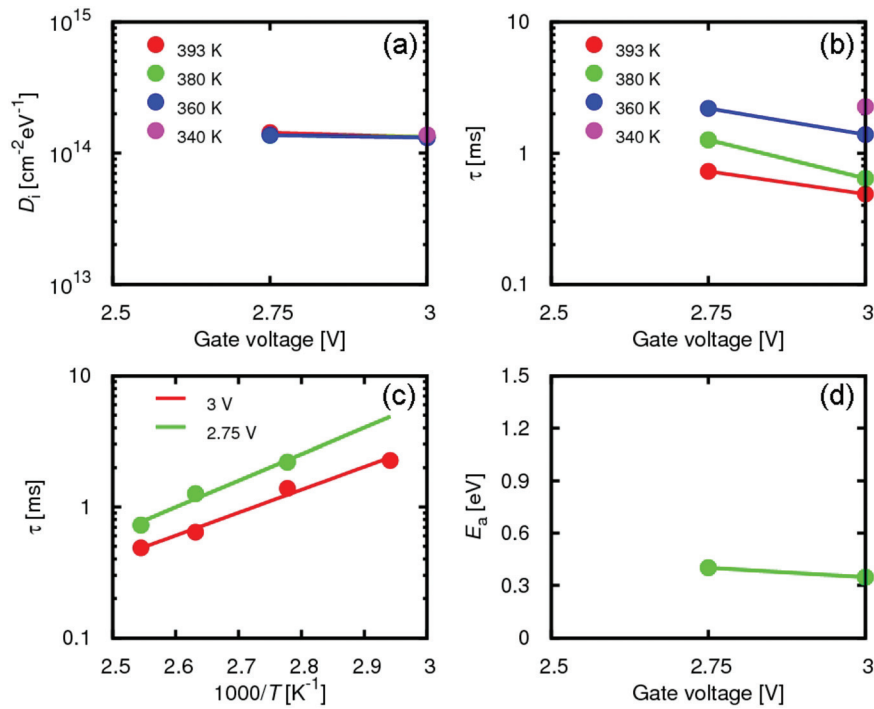


FIG. 4. (a) Interface state density D_i and (b) electron trapping time constant τ , obtained from the peak values and positions of the frequency-dependent G_i/ω based on the conductance method. (c) The Arrhenius plot of the temperature-dependent τ . (d) The activation energy E_a as a function of gate voltage, obtained from the Arrhenius plot (c).

where q is the electron charge and $\omega = 2\pi f$ is the angular frequency; G_i/ω as a function of frequency exhibits a single-peaked behavior, with the peak frequency $\sim 1/\pi\tau$ and the

peak value $\sim 0.4q^2D_i$. Assuming the designed value of the insulator capacitance $C_0 = 610 \text{ nF/cm}^2$, we show frequency dependence of G_i/ω , for several temperatures and gate voltages of 0 V, 1.5 V, and 3 V, in Fig. 3. As the gate voltage decreases, the number of peaks decreases due to longer time constants for deeper interface state energy levels. Thus, only a narrow range of the gate biases gives peaks in the measured frequency and temperature range; most peaks are below

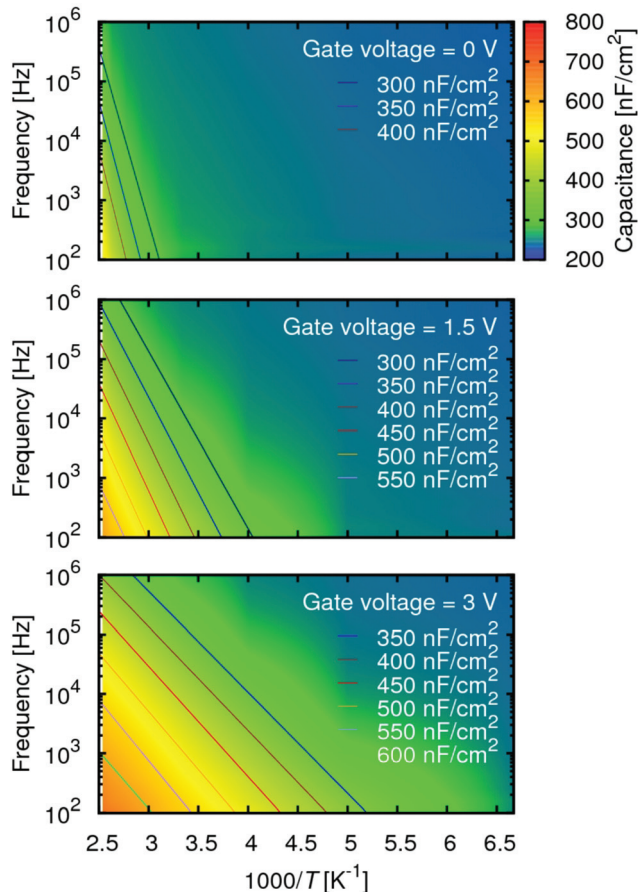


FIG. 5. C - f - T mappings with contours at gate voltages of 0 V (top), 1.5 V (middle), and 3 V (bottom).

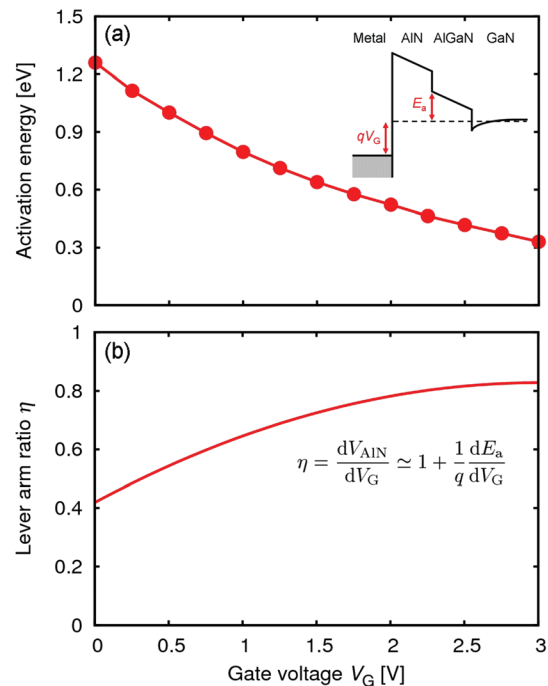


FIG. 6. (a) Gate voltage V_G dependence of the activation energy E_a extracted from the contours in C - f - T mappings. Inset: illustration of the bandbending and E_a . (b) Lever arm ratio $\eta = dV_{\text{AIN}}/dV_G \approx 1 + q^{-1}dE_a/dV_G$.

100 Hz due to significantly long time constants for the wide bandgap of AlGaIn/GaN systems. From the few peak positions and values, D_i and τ for temperatures of 340–393 K are obtained as shown in Figs. 4(a) and 4(b), respectively, where $D_i \sim 10^{14} \text{ cm}^{-2} \text{ eV}^{-1}$ and $\tau \sim \text{ms}$. From the Arrhenius plot of the temperature dependence of τ shown in Fig. 4(c), given by $\tau = \tau_0 \exp(E_a/k_B T) = \tau_0 \exp(\beta E_a)$, we extracted the activation energy E_a shown in Fig. 4(d) and estimated $\tau_0 \sim 10 \text{ ns}$. However, we have a problem that the conventional conductance method to investigate interface states is available only for a narrow range of gate biases, prohibiting the analysis of deeper interface states.

In order to solve the problem, we propose an analysis method using C - f - T mapping obtained from the temperature-dependent C - V - f characteristics. In Fig. 5, we show the C - f - T mappings at gate voltages of 0 V, 1.5 V, and 3 V, with contours. The contours exhibit a straight line behavior, which can be explained by the equivalent circuit of the MIS structures with a total admittance

$$Y = \frac{1}{Z} = \left(\frac{1}{jC_0\omega} + \frac{1}{G_i + jC_s\omega + jC_i\omega} \right)^{-1}. \quad (3)$$

Since C_i given by Eq. (1) and G_i/ω by Eq. (2) are functions of only $\omega\tau$, the measured capacitance $C = \text{Im}Y/\omega$ is a function of only $\omega\tau$. Therefore, a contour in C - f - T mapping, i.e., $C = \text{constant}$ leading to $\omega\tau = 2\pi f\tau = \text{constant}$, exhibits a straight line behavior as expressed by $f \propto 1/\tau \propto \exp(-\beta E_a)$, from which the activation energy E_a corresponding to the interface state energy level can be extracted. Figure 6(a) shows the gate voltage V_G dependence of E_a extracted from the contours in the C - f - T mappings, with the inset illustrating the bandbending and E_a . In addition to the fact that the obtained values of E_a for the gate voltage $\geq 2.75 \text{ V}$ are in good agreement with those obtained by the conductance method, we find that E_a can be obtained for a much extended range of the gate biases. This is due to slow $\omega\tau$ dependence of Eqs. (1) and (2); even though the frequency is far from the peak position $\sim 1/\pi\tau$, change in the C - f - T mapping is detectable. Furthermore, from the interface state energy levels corresponding to a wide range of the gate biases, the gate-control efficiency of the devices can be directly evaluated from the derivative dE_a/dV_G . As shown in the inset of Fig. 6(a), the gate voltage change ΔV_G is divided by the AlN gate insulator with ΔV_{AIN} and AlGaIn/GaN. Since $\Delta V_G \simeq \Delta V_{\text{AIN}} - \Delta E_a/q$, we obtain a “lever arm ratio” $\eta = dV_{\text{AIN}}/dV_G \simeq 1 + q^{-1}dE_a/dV_G$ as shown in Fig. 6(b). We find that small negative values of dE_a/dV_G give large values of η near the unity corresponding to poor gate-control efficiencies. This analysis method is important as an auxiliary tool to the conventional conductance method.

In summary, we analyzed the AlN/AlGaIn/GaN MIS-HFETs using C - f - T mapping for the investigation of AlN/AlGaIn interface states. The analysis method gives the activation energies of electron trapping, namely the interface

state energy levels, for a wide range of the gate biases. This method is auxiliary to the conventional conductance method, serving as a valuable tool for characterization of wide-bandgap devices with deep interface states. Furthermore, the method also enables a direct evaluation of the gate-control efficiency of the devices.

- ¹M. Khan, A. Bhattacharai, J. Kuznia, and D. Olson, *Appl. Phys. Lett.* **63**, 1214 (1993).
- ²T. Hashizume, S. Ootomo, and H. Hasegawa, *Appl. Phys. Lett.* **83**, 2952 (2003).
- ³C. Liu, E. F. Chor, and L. S. Tan, *Appl. Phys. Lett.* **88**, 173504 (2006).
- ⁴A. Kawano, S. Kishimoto, Y. Ohno, K. Maezawa, T. Mizutani, H. Ueno, T. Ueda, and T. Tanaka, *Phys. Status Solidi C* **4**, 2700 (2007).
- ⁵K. Saito, T. Ono, M. Shimada, N. Shigekawa, and T. Enoki, *Jpn. J. Appl. Phys.* **44**, 334 (2005).
- ⁶M. Kudo, H.-A. Shih, M. Akabori, and T. Suzuki, *Jpn. J. Appl. Phys.* **51**, 02BF07 (2012).
- ⁷Y. Liu, J. A. Bardwell, S. P. McAlister, S. Rolfe, H. Tang, and J. B. Webb, *Phys. Status Solidi C* **0**, 69 (2002).
- ⁸J. Hwang, W. Schaff, B. Green, H. Cha, and L. Eastman, *Solid-State Electron.* **48**, 363 (2004).
- ⁹N. Tanaka, H. Takita, Y. Sumida, and T. Suzuki, *Phys. Status Solidi C* **5**, 2972 (2008).
- ¹⁰N. Tanaka, Y. Sumida, H. Kawai, and T. Suzuki, *Jpn. J. Appl. Phys.* **48**, 04C099 (2009).
- ¹¹N. Tsurumi, H. Ueno, T. Murata, H. Ishida, Y. Uemoto, T. Ueda, K. Inoue, and T. Tanaka, *IEEE Trans. Electron Devices* **57**, 980 (2010).
- ¹²S. Huang, Q. Jiang, S. Yang, C. Zhou, and K. Chen, *IEEE Electron Device Lett.* **33**, 516 (2012).
- ¹³G. Slack, R. Tanzilli, R. Pohl, and J. Vandersande, *J. Phys. Chem. Solids* **48**, 641 (1987).
- ¹⁴R. Stoklas, D. Gregušová, Š. Gaží, J. Novák, and P. Kordoš, *J. Vac. Sci. Technol. B* **29**, 01A809 (2011).
- ¹⁵H.-A. Shih, M. Kudo, M. Akabori, and T. Suzuki, *Jpn. J. Appl. Phys.* **51**, 02BF01 (2012).
- ¹⁶L. Lipkin and J. Palmour, *IEEE Trans. Electron Devices* **46**, 525 (1999).
- ¹⁷T. Adam, J. Kolodzey, C. Swann, M. Tsao, and J. Rabolt, *Appl. Surf. Sci.* **175–176**, 428 (2001).
- ¹⁸M.-A. Dubois and P. Mural, *Appl. Phys. Lett.* **74**, 3032 (1999).
- ¹⁹Y. Chiou, S. Chang, Y. Su, C. Wang, T. Lin, and B.-R. Huang, *IEEE Trans. Electron Devices* **50**, 1748 (2003).
- ²⁰M. Miczek, C. Mizue, T. Hashizume, and B. Adamowicz, *J. Appl. Phys.* **103**, 104510 (2008).
- ²¹C. Mizue, Y. Hori, M. Miczek, and T. Hashizume, *Jpn. J. Appl. Phys.* **50**, 021001 (2011).
- ²²E. J. Miller, X. Z. Dang, H. H. Wieder, P. M. Asbeck, E. T. Yu, G. J. Sullivan, and J. M. Redwing, *J. Appl. Phys.* **87**, 8070 (2000).
- ²³R. M. Chu, Y. G. Zhou, K. J. Chen, and K. M. Lau, *Phys. Status Solidi C* **0**, 2400 (2003).
- ²⁴L. Semra, A. Telia, and A. Soltani, *Surf. Interface Anal.* **42**, 799 (2010).
- ²⁵B. Gaffey, L. Guido, X. Wang, and T. Ma, *IEEE Trans. Electron Devices* **48**, 458 (2001).
- ²⁶R. Stoklas, D. Gregušová, J. Novák, A. Vescan, and P. Kordos, *Appl. Phys. Lett.* **93**, 124103 (2008).
- ²⁷J. J. Freedman, T. Kubo, and T. Egawa, *Appl. Phys. Lett.* **99**, 033504 (2011).
- ²⁸T. Mizutani, H. Makihara, M. Akita, Y. Ohno, S. Kishimoto, and K. Maezawa, *Jpn. J. Appl. Phys.* **42**, 424 (2003).
- ²⁹M. Faqir, G. Verzellesi, F. Fantini, F. Danesin, F. Rampazzo, G. Meneghesso, E. Zanoni, A. Cavallini, A. Castaldini, N. Labat, A. Touboul, and C. Dua, *Microelectron. Reliab.* **47**, 1639 (2007).
- ³⁰Y. Nakano and T. Jimbo, *Appl. Phys. Lett.* **80**, 4756 (2002).
- ³¹T. Okino, M. Ochiai, Y. Ohno, S. Kishimoto, K. Maezawa, and T. Mizutani, *IEEE Electron Device Lett.* **25**, 523 (2004).
- ³²E. H. Nicollian and J. R. Brews, *MOS (Metal Oxide Semiconductor) Physics and Technology* (Wiley-Interscience, Hoboken, New Jersey, 1982).
- ³³K. Lehovec, *Appl. Phys. Lett.* **8**, 48 (1966).